Bull. Mater. Sci., Vol. 39, No. 2, April 2016, pp. 365–376. © Indian Academy of Sciences.

Preparation and characterization of Li_2O–CaO–Al_2O_3–P_2O_5–SiO_2 glasses as bioactive material

HIMANSHU TRIPATHI*, AREPALLI SAMPATH KUMAR and S P SINGH
Department of Ceramic Engineering, Indian Institute of Technology (BHU), Varanasi 221 005, India

MS received 16 April 2015; accepted 29 October 2015

Abstract. **The aim of the present investigation was to study the role of Al_2O_3 in the Li_2O–CaO–P_2O_5–SiO_2 bioactive glass for improving the bioactivity and other physico-mechanical properties of glass. A comparative study on structural and physico-mechanical properties and bioactivity of glasses were reported. The structural properties of glasses were investigated by X-ray diffraction, Fourier transform infrared spectrometry, scanning electron microscopy and the bioactivity of the glasses was evaluated by *in vitro* test in simulated body fluid (SBF). Density, compressive strength, Vickers hardness and ultrasonic wave velocity of glass samples were measured to investigate physical and mechanical properties. Results indicated that partial molar replacement of Li_2O by Al_2O_3 resulted in a significant increase in mechanical properties of glasses. *In vitro* studies of samples in SBF had shown that the pH of the solution increased after immersion of samples during the initial stage and then after reaching maxima it decreased with the increase in the immersion time. *In vitro* test in SBF indicated that the addition of Al_2O_3 up to 1.5 mol% resulted in an increase in bioactivity where as further addition of Al_2O_3 caused a decrease in bioactivity of the samples. The biocompatibility of these bioactive glass samples was studied using human osteoblast (MG-63) cell lines. The results obtained suggested that Li_2O–CaO–Al_2O_3–P_2O_5–SiO_2-based bioactive glasses containing alumina would be potential materials for biomedical applications.**

Keywords. **Mechanical characterization; glass; biomaterials; FTIR; SEM.**

1. Introduction

Bioactive glasses have been widely investigated for bone repair because of their outstanding bioactive properties. However, bioactive materials undergo incomplete conversion into a bone-like material which limits their biomedical application [1]. In simulated body fluid (SBF), bioactive glasses bind to living bone through an apatite layer formed on their surfaces [2]. The bonding mechanism of implant to the bone was given by Clark and Hench [3]. Hench decided to make a glass of the SiO_2–Na_2O–CaO–P_2O_5 system containing high calcium contents with a composition close to a ternary eutectic in the Na_2O–CaO–SiO_2 diagram [4]. The main discovery was that a glass of the mol% composition 46.1 SiO_2–24.4 Na_2O–26.9 CaO–2.6 P_2O_5, known as 45S5 bioglass, formed a strong bond with bone which could not be removed without breaking the bone [5]. This launched the field of bioactive ceramics with many new materials and products [4,6,7]. 45S5 is widely used in biomedical devices such as middle ear and dental implants. However, relatively low strength and brittleness limits its application to non-load-bearing situations [8]. Interest has also increased in borate glasses mainly due to very encouraging clinical results of healing the harmful chronic wounds like diabetic and ulcers [9,10]. The benefits of phosphate glasses are related to their very rapid solubility like borate glasses rather than bioactivity [11].

The 45S5 glass tends to crystallize at high temperature like other bioactive glasses owing to its relatively low silica content [12]. It was a relevant drawback because the crystallization had reduced the bioactivity of the glass [13,14]. The addition of elements like magnesium, aluminium, zirconia or titanium may be used to control some physical and chemical properties of bioglasses [15,16]. Many systematic investigations have been carried out by earlier workers to check the effect of alumina on bioactivity and mechanical properties of phosphate, silicate and phosphor silicate-based bioglasses, and bioglass-ceramics, whereas the role of Al_2O_3 for Li_2O has never been investigated in such systems [17]. The addition of Al_2O_3 to the bioactive glass is expected to improve the repair in bone defect and to control the degradation rate for long-term stability of the implants. Sitarz *et al* [18] have observed that the addition of Al^{3+} in proper concentration increased the mechanical resistance of the bioglasses. The presence of Al_2O_3 results in the breaking of P=O bonds and the Si–O–P linkages are replaced by Al–O–P linkages in the glass network which prevents the degradation [19]. However, the addition of Al_2O_3 in higher concentrations to the borate-free silicate-based bioactive glass is not desirable due to the ability to damage the genome or to disrupt the cellular metabolic processes and harmful impact on the bioactivity of glass [20,21]. In recent years, the earlier work has shown the increasing effect of lithium on bone density.

*Author for correspondence (himanshutripath@gmail.com, himanshu.tripathi.rs.cer@itbhu.ac.in)

Table 1. Mol% composition of the bioglass samples.

Samples	SiO_2	CaO	P_2O_5	Li_2O	Al_2O_3	Al_2O_3/Li_2O ratio
LiAl0.0	42	34	6	18	0	0.00
LiAl0.5	42	34	6	17.5	0.5	0.028
LiAl1.0	42	34	6	17	1.0	0.058
LiAl1.5	42	34	6	16.5	1.5	0.090
LiAl2.5	42	34	6	15.5	2.5	0.161

The anabolic effect of lithium on the mass density of bone in mice had shown by Clement-Lacroix *et al* [22]. The maintenance therapy with lithium can safely preserve and intensify bone density as earlier reported by Zamani *et al* [23].

Although the role of Al_2O_3 in glass is commonly different from that of Li_2O but the molar addition of 0.5–2.5 mol% Al_2O_3 for Li_2O in glass was carried out on the basis of the earlier concepts in order to improve the required properties of the glass. The purpose of substitution of Al_2O_3 for Li_2O is to improve the structural properties and the bioactivity of the glass and prepare a bioactive glass which can be mechanically as well as hydrolytically stable as an implant material. The aim of this work in other words is to provide information on assessment of bioactivity through *in-vitro* test in SBF and to increase the physio-chemical as well as mechanical properties of base bioactive glass by introducing 0.5–2.5 mol% Al_2O_3 into it. Therefore, in the present investigation, the concentration of Li_2O was varied by mol% addition of Al_2O_3 from 0.5 to 2.5.

2. Experimental

2.1 *Materials and methods*

The mol% compositions and ratio of Al_2O_3 to Li_2O of the bioglass samples have been given in table 1. Fine-grained quartz was used as a source of SiO_2. Analytical reagent grades $CaCO_3$, Li_2CO_3 and $(NH_4)H_2PO_4$ were used as a source of CaO, Li_2O and P_2O_5, respectively. The required amounts of analytical reagent grade Al_2O_3 were added in the batch for the partial substitution of Li_2O. The raw materials for different samples were properly weighed. Then the mixing of different batches was done for 30 min and after that, they were melted in a 100 ml platinum–2% rhodium crucible at 1400°C in the air as furnace atmosphere. The temperature of the furnace was controlled within ±10°C by an automatic temperature indicator-cum controller. The thermal cycle was set for the all glass samples from room temperature to 1000°C at the 10°C min^{-1}. Further, it was held at 1000°C for 1 h and heated from 1000 to 1400°C at the rate of 10°C min^{-1} and again held at 1400°C for 2 h. The melting of samples was done in the electric globar furnace in air as the furnace atmosphere. The melted samples were poured on a preheated aluminium sheet and directly transferred to a regulated muffle furnace at 450°C for annealing.

Table 2. Ions concentration in SBF solution.

Ion	Concentration (mM)
Na^+	142.0
K^+	5.0
Mg^{2+}	1.5
Ca^{2+}	2.5
Cl^-	147.8
HCO_3^-	4.2
HPO_4^{2-}	1.0
SO_4^{2-}	0.5

After 1 h of annealing of the samples, the furnace was cooled to the room temperature at the controlled rate of cooling. The samples were crushed in a pestle mortar and then ground in an agate mortar to make fine powders of the samples for different properties measurements by different experimental techniques.

2.2 *In vitro analysis in SBF*

The glass samples prepared were immersed in SBF solution at 37.4°C for different time periods varying from 1 to 28 days. The SBF solution was prepared according to the formula described by Kokubo *et al* [24]. Table 2 shows the ion concentration in SBF solution. The pH of the SBF solution was measured using a digital pH meter after immersion of samples for different time periods.

2.3 *Structural analysis of bioglasses by Fourier transform infrared (FTIR) reflectance spectroscopy*

The *in-vitro* bioactivity of chemically treated samples in SBF solution was assessed by evaluating the formation of carbonated hydroxy calcium phosphate layer on the surface of the samples before and after immersion in SBF solution using FTIR diffuse reflectance spectrometry. KBr powder was used as a reference during spectral reflectance measurement. Briefly, 64 scans for KBr background and 64 scans for each powdered samples were made with signal gain 1. The resolution was 4 cm^{-1}. The infrared reflectance spectra of the bioglasses were recorded at the room temperature in the spectral range 4000–400 cm^{-1} using an FTIR diffuse reflectance spectrometer (Nicolet iS10, Thermofisher, USA) and the reflectance spectra were converted to absorption mode by plotting log $(1/R)$ against wavenumbers as shown in figure 10a–d.

2.4 *Microstructure analysis using scanning electron microscope (SEM)*

The surfaces of bioactive glasses were analysed before and after immersion in SBF solution by SEM. The samples

were gold coated before SEM analysis. A SEM (Inspect 50 FEI) was used for determining the surface microstructure of bioactive glass samples.

2.5 *Density, compressive strength and ultrasonic wave velocity measurements*

The densities of the samples were determined by Archimedes's principle with water as the immersion liquid. The measurements were carried out at room temperature. Compressive strength of bioactive glass samples was measured by universal testing machine. Young's modulus, shear modulus and bulk modulus of glass samples were determined by ultrasonic measurement gauge. The ultrasonic wave velocities were recorded as longitudinal (V_L) and transverse wave (V_T). The velocities of sound wave propagated in the polished bioglass samples were measured using ultrasonic pulse-echo techniques (EPOCH-600 Olympus, USA). The test was performed using two transducers, one was V112 for longitudinal wave (10 MHz) and another was V156 for the transverse wave (5 MHz). Burnt honey was used as bonding material between samples and transducers. Elastic properties such as Poisson's ratio (σ), Young's modulus (E), shear modulus (S) and bulk modulus (K) using the following standard equations:

$$\text{Poisson's ratio } (\sigma) = \frac{1 - 2\,(V_T/V_L)^2}{2 - 2\,(V_T/V_L)^2}, \tag{1}$$

$$\text{Young's modulus } (E) = \frac{V_L^2 \rho\,(1+\sigma)\,(1-2\sigma)}{1-\sigma}, \tag{2}$$

$$\text{Shear modulus } (G) = V_T^2 \rho, \tag{3}$$

$$\text{Bulk modulus } (K) = \frac{E}{3\,(1-2\sigma)}, \tag{4}$$

where ρ is the density of glass sample.

2.6 *Vickers hardness*

The microhardness of the bioglass samples were measured by using the Vickers microhardness tester (test load at 0.98 N m^{-2} and dwell time 10 s) HMV-FA, SHIMADZU, Japan. The procedure adopted for this test is according to the ASTM-E384 standard. The Vickers hardness was determined using the formula

$$HV = 1854.4P/d^2, \tag{5}$$

where the load P is in N m^{-2} and diagonal d is in μm.

2.7 *In-vitro biocompatibility study*

The *in-vitro* cell viability and cytotoxicity of bioactive glass samples against osteoblast (MG63) cell lines have been performed in order to assess the biocompatibility. The human osteoblast MG63 cell lines (ATCC, USA) were used in this investigation. The bioactive glass samples were sterilized in an autoclave at 121°C for 30 min. MG63 cells were cultured in a minimum essential medium (MEM; Invitrogen Corporation), augmented with 10% of foetal calf serum (FCS), 1% antibiotic antimycotic solution in a humidifed atmosphere at 37°C and with 5% CO_2 for 24, 48 and 72 h. The methyl thiazolyl tetrazolium (MTT) [3-(4,5-dimethylthiazol-2-yl)-2,5-diphenyl tetrazolium bromide] assay was used for evaluating the cell viability [25] and cytotoxicity [26].

3. Results and discussion

3.1 *Mechanical properties*

3.1a *Density and compressive strength*: Figures 1 and 2 show the density and compressive strength of the glass samples as a function of Al_2O_3/Li_2O ratio. From figure 1 it is

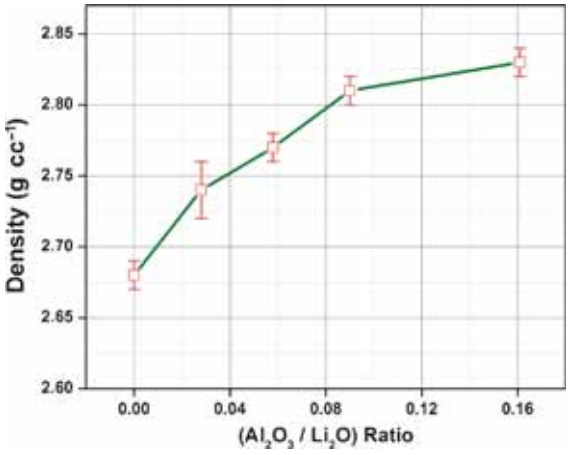

Figure 1. Variation in density with Al_2O_3/Li_2O ratio in bioglass samples LiAl0.0 to LiAl2.5.

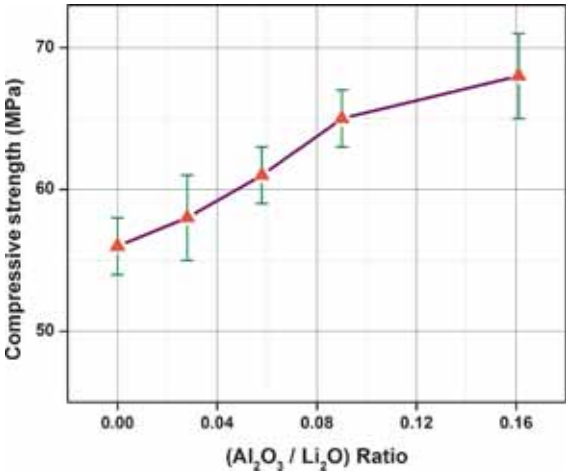

Figure 2. Variation in compressive strength with Al_2O_3/Li_2O ratio in bioglass samples LiAl0.0 to LiAl2.5.

clear that an increase in Al_2O_3 substitution up to 1.0 mol% resulted in an increase in the density of glass samples from 2.68 to 2.77 g cm^{-3} but further beyond that up to 2.5 mol% it tends to saturate at 2.83 g cm^{-3} in the glass. This is attributed due to the reason that lighter element lithium has been replaced by heavier element aluminium up to a limited substitution of 1.0 mol% Al_2O_3. However, the tendency towards saturation of density beyond 1.0 mol% Al_2O_3 can be due to compensating free volume increase with the increase in aluminium leading to asymptotic behaviour of density changes in the glass samples. On the other hand, the compressive strength of the glass system has also been found to increase with the increase in Al_2O_3/Li_2O ratio in the glass (figure 2) as the bigger Li^+ ion (0.59 Å) has been replaced by a smaller Al^{3+} ion (0.39 Å) in tetrahedral co-ordination [27] in the glass system. It was expected that the low expansion produced by smaller Al^{3+} ion had resulted a high surface compression giving high strength in the bioactive glass samples. Chemical strengthening of glass by ion exchange process is done not only by replacement of a smaller ion by a bigger ion but also *vice-versa* with an exchange of a bigger ion by a smaller ion in the glass [28]. Although the role of Al_2O_3 as an intermediate oxide in the glass structure has been reported to be different from that of alkali oxides as modifiers but substitution of Li_2O for Al_2O_3 in glass has been reported by earlier workers [29–31].

3.1b *Elastic modulus, shear modulus and bulk modulus*: Figure 3 shows an increase in the elastic modulus, shear modulus and bulk modulus with the increase in Al_2O_3/Li_2O ratio in the glass samples. The figure 3 also represents the experimental values of the elastic moduli, Young's modulus (E), shear modulus (S) and bulk modulus (K) of the bioglasses. All the elastic moduli values were found to increase with the increase in Al_2O_3/Li_2O ratio. The elastic moduli of the bioglass samples show similar trends regarding improvement in their mechanical properties with the variations in the ultrasonic velocities.

Young's modulus dictates the stiffness of materials, which is also attributed to the greater bond strength between the atoms in a material. Hence, higher Young's modulus, greater the stiffness of the material and closer would be the bonding [32]. As shown in figure 3 that an increase in Young's modulus, shear modulus and bulk modulus of the bioglass samples is due to increase in bridging oxygens (–O–) by the addition of Al_2O_3 in the glass structure which is also evident from the FTIR absorption bands observed at 432 and 745 cm^{-1} for AlO_6 and AlO_4 units (figure 10a). On increasing the concentration of Al_2O_3 beyond 1.5 mol%, AlO_4 units prevail in the glass matrix which results in an increase in the number of bridging oxygens. Thus bridging oxygens (–O–) have improved the connectivity of the glass network. Earlier, it has been also shown that the addition of Al_2O_3 for Na_2O in a sodium silicate glass has increased Young's modulus of the glass [33]. Thus, the structure of glass becomes more rigid and stiff which resulted in an increase in Young's modulus from 90.47 to 104.38 GPa with the increase in Al_2O_3 content in the base bioglass. Further, an increase in shear modulus (35.90 to 41.91 GPa) and bulk modulus (64.91–79.72 GPa) has also confirmed the improvement in elastic properties of the glass samples.

3.1c *Vickers hardness*: It can be seen from figure 4 that the Vickers hardness of the bioglass samples has increased gradually as Al_2O_3/Li_2O ratio increased. The mean values of the Vickers hardness of samples have been taken with several trials and presented in the form of error bars. Since the binding energy (Columbic force $= ZZ'/(r + r_0)^2$ where Z and Z' are the charge on the cations and O^{2-} ion; r and r_0 are ionic radii of cations and O^{2-} ion, respectively) between Al^{3+} and

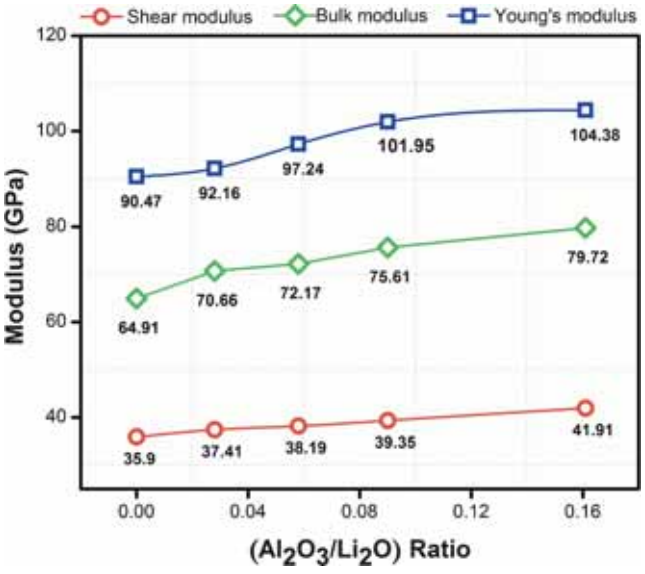

Figure 3. Elastic modulus, shear modulus and bulk modulus of all bioglass samples.

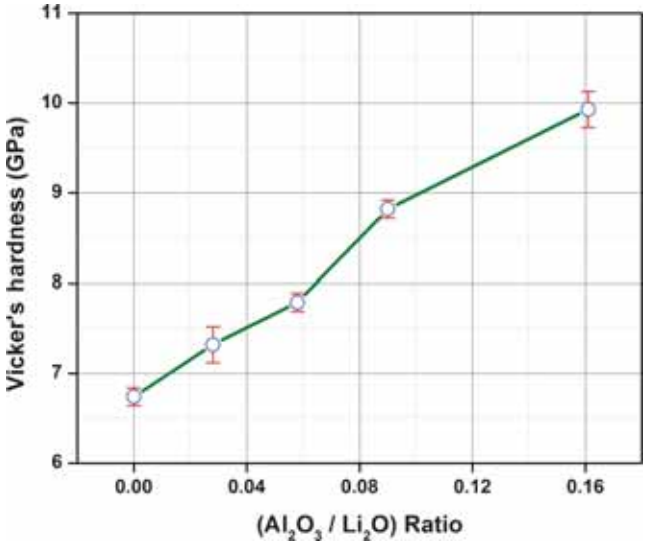

Figure 4. Vickers hardness of the bioglass samples.

O^{2-} ions have increased comparatively more than Li^+ and O^{2-} ions in the glass resulting in bond strengthening with the Al_2O_3 addition. It is mentioned herewith that the replacement of bigger Li^+ by smaller Al^{3+} ion has not only increased the bond strength by increasing the multiple of charge (ZZ') but the same has also resulted in strengthening due to smaller ionic radii of Al^{3+} than Li^+ ion. This would naturally compress the structure and thus improving the hardness of the glass samples [34]. Hence replacement of lithia by alumina on molar basis had enhanced the mechanical properties of the bioglass samples as also evident from the results presented in figures 1–4. Therefore, it increased the densities and resulted in creating new bonds with the incorporation of aluminium ions. It has caused reinforcement of the glass structure and resulted in improvement in the compression of the glass and thus preventing the penetration in the glass system. Same time the alumina is well known to prevent the devitrification of glass and also it increases tremendously the chemical durability of glasses [35,36]. That is why the Vickers hardness of the bioglass samples had increased with increasing amount of Al_2O_3 in glass.

El-Kheshen *et al* [17] have also investigated the effect of Al_2O_3 addition on bioactivity and mechanical properties of soda-lime-alumino-phosphate bioactive glasses and found that Al_2O_3 has appreciably increased the hardness of the glass. Sitarz *et al* [19] have also studied influence of alumina on the structure and texture of alkali–alkaline earth-phosphosilicate and alkali-alkaline earth-alumino-phospho-silicate glasses and spectroscopically established its homogenizing effect on structure of glass. The authors have mentioned that addition of small amount of alumina (5 mol% of $AlPO_4$) has caused a change in composition of the glassy matrix and inclusions and thereby making it mechanically more stable. The observations made by earlier workers [17–19] support our present results regarding improvement of mechanical properties of bioglasses by substitution of alumina at the cost of lithia.

3.2 *pH behaviour of the samples in SBF solution*

Figure 5 shows the variation of pH of bioactive glass samples after immersing in SBF solution up to 28 days. It shows that for all bioactive glass samples, the pH increases within 1–3 days as compared to the initial pH of the SBF solution at 7.4 under physiological condition. The increase in pH values is due to fast release of cations through exchange with H^+ or H_3O^+ ions in the SBF solution. The H^+ ions are being replaced by cations which cause an increase in hydroxyl concentration of the solution [37]. This leads to attack on the silica glass network, which results in silanols formation leading to decrease in pH after 3 days as indicated in figure 5 when bioactive glass samples were immersed in SBF solution up to 28 days. The change in pH was due to leaching of cations. The increase in pH of SBF solution shows a decrease in the concentration of H^+ ions due to the replacement of cations in the bioactive glasses. Figure 5 shows that the addition of alumina up to 1.5 mol% resulted in an

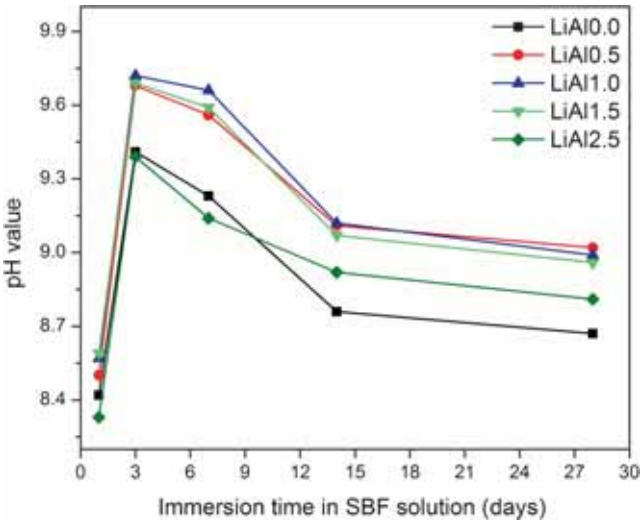

Figure 5. Variation of pH of bioactive glass samples after immersing in simulated body fluid (SBF) up to 28 days.

increase in pH of the SBF solution containing immersed samples which attained maxima after around 3 days and then it decreased with time referring to base glass sample. The high degradation rate leads to higher pH value. Hence, an increase in the pH value of SBF solution also favours the hydroxy carbonate apatite formation. However, the addition of Al_2O_3 beyond 1.5 mol% caused a decrease in maxima of the pH of SBF solution containing immersed sample. This dictates that the addition of Al_2O_3 up to 1.5 mol% in the glass samples has increased its bioactivity, but beyond 1.5 mol% of Al_2O_3 retards the bioactivity of the glass samples (figure 5). This observation can be explained in the manner that the addition of Al_2O_3 up to 1.5 mol% goes into the formation of AlO_6 octahedra and produces more of non-bridging oxygens which results in an increase in bioactivity of samples. Whereas further addition of Al_2O_3 beyond 1.5 mol% results in the formation of AlO_4 tetrahedra which causes a decrease in the bioactivity of the samples. However, previous investigations made by Belkebir *et al* [38] had pointed out that AlO_6 octahedra dominated the glass structure when Al_2O_3 was present in small concentrations, but AlO_4 tetrahedral units prevailed when Al_2O_3 concentration was higher. MAS NMR studies made earlier in glasses with [27] Al by Muller *et al* [39] and Brow *et al* [40] have revealed that aluminium ions occupy both tetrahedral sites with AlO_4 network former and octahedral with AlO_6 network modifier in the structure according to their suggested mechanism. Hence, the AlO_4 tetrahedra increases the strength of the glass and also AlO_6 octahedra increases the bioactivity of the bioglass samples. Greenspan *et al* [41] also confirmed that the change in pH of glass samples took place after immersion in SBF solution. Morphological properties of bioactive glasses also indicate that soaking in SBF solution leads to the formation of hydroxyapatite layer on the surface of the samples [42,43].

The maxima of pH values were recorded on the third days as pH = 9.41, 9.68, 9.72, 9.69 and 9.39 for the samples LiAl0.0 to LiAl2.5, respectively, at 37°C under physiological

condition, which is due to the fast dissolution rate. The addition of Al_2O_3 up to 1.5 mol% the maxima of pH is more than the base glass, but beyond that it is lower than the base glass sample. This may influence the formation of the apatite layer on the surface of the glass samples at an early stage [44]. The earlier investigations done by Majhi *et al* [45] regarding the pH behaviour of SBF solution containing immersed bioglass and bioglass ceramic samples has also confirmed the formation of hydroxy carbonate apatite layer on the surface of the samples showing its bioactivity. In the initial stages the authors found that the pH of the solution increased with the increase in immersion time which attained maxima and then it decreased continuously with increasing time. This confirms that the bioactivity of a particular sample attains maxima only after a specific period of time which shows its maximum bioactivity at this point of time. The maxima in bioactivity were found to vary from one sample to another depending upon the bioglass and bioglass ceramic compositions [46,47]. When bone is formed, the cross linking of the collagen chains and the subsequent precipitation of hydroxyl carbonate apatite is pH dependent and require a high pH at the bone formation site [48]. Ohtsuki and Kokubo [20] had earlier investigated the effect of Al_2O_3 on bioactivity of $CaO–SiO_2–Al_2O_3$ glasses by *in vitro* tests. They evaluated the bioactivity of the glass samples by hydroxy apatite formation on the surface of these glasses using various instrumental techniques and found that calcium aluminosilicate containing less than 1.5 mol% Al_2O_3 formed the apatite layer on the surface of the glass, but glasses containing more than 1.7 mol% of Al_2O_3 did not form this layer. The authors [20] have mentioned with well known fact that glasses and glass ceramics form interfacial bonds with living bone due to the formation of an apatite layer on the surface of these systems. The apatite layer on the surface can be reproduced even in acellular SBF which has almost equal concentrations of ions to those of human blood plasma. Moreover, Bohmer and Lematre [2] after critical review had also mentioned the *in vitro* method for testing the extent of bone bonding of a biomaterial and they said that it was a very attractive concept. The results of the present investigations entirely based on the well-established *in vitro* tests are well supported by earlier studies [20,46,47].

3.3 *In vitro bioactivity of bioglasses by X-ray diffractometry*

X-ray diffraction (XRD) patterns were observed using a Rigaku portable XRD machine (Rigaku, Tokyo, Japan). Phase identification analysis was carried out by comparing the XRD patterns of the bioactive glass samples to the standard database stated by JCPDS. Figure 6 shows the XRD patterns of the bioactive glass samples before soaking them into the SBF. Before being soaked in SBF solutions, there was no XRD absorption peak for the bioactive glass samples, except a bump like peak ranging from 20° to 30°, which is due to Si–O–Si network. So, it is clear that bioactive glass samples were amorphous in nature before being soaked in SBF solution. Figure 7 shows the XRD patterns of the bioactive glass samples soaked in the SBF solution for 14 days. After being soaked in the SBF solution for 14 days, one broad diffraction peak was observed at 30–32° of 2θ angle, corresponding to the HA phase [48]. These peaks were identified by standard JCPDS cards numbered 89-6495. In fact, the XRD patterns of bioglass samples which have broad 'humps' centred around $2\theta = 31°$, confirm the amorphous nature of the hydroxy carbonate apatite [49].

3.4 *SEM analysis of bioactive glass samples*

The SEM micrographs of bioactive glass samples before soaking in SBF solution are shown in figure 8a–e which

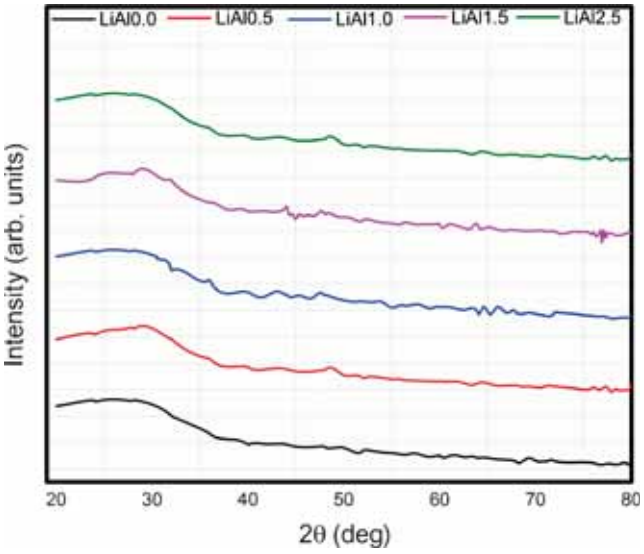

Figure 6. XRD patterns of the bioactive glass samples before soaking them into the simulated body fluid solution.

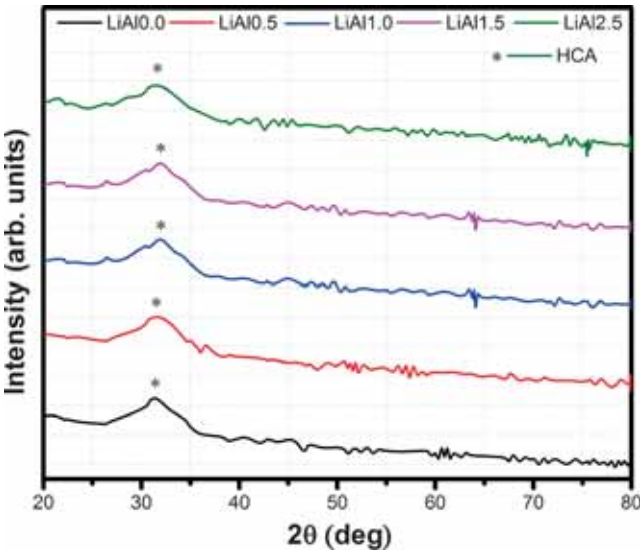

Figure 7. XRD patterns of the bioactive glass samples soaked in the simulated body fluid solution for 14 days.

shows different rod type structure and irregular grain of bioactive glass samples which are quite similar to the result found by Hanan *et al* [50]. Figure 9a–e shows the SEM micrographs of bioactive glass samples after soaking in SBF solution for 28 days. It is clear from figure 9 that bioactive glass samples which were soaked in SBF solution for 28 days were covered with irregular shape and grounded HA particles have been grown into several agglomerates consisting of HA layer. These micrographs show the formation of HA on the surface of bioactive glass samples after immersion in SBF solution for 28 days.

3.5 *FTIR spectrometry*

Figure 10a–d shows the FTIR absorption spectra of various bioglass samples for a plot of $\log(1/R)$ *vs.* wavenumber before and after soaking them into SBF solution for different time intervals. Figure 10a shows the absorption spectra of all bioglass samples before soaking them in SBF solution. The FTIR spectra of glass samples before immersion in SBF solution exhibit vibrational bands at around 432 cm^{-1} due to Si–O–Si bending/AlO_6 units and 635 cm^{-1} due to Si–O–Si bending [51,52], 870, 970 and 1200 cm^{-1} due to Si–O–Si

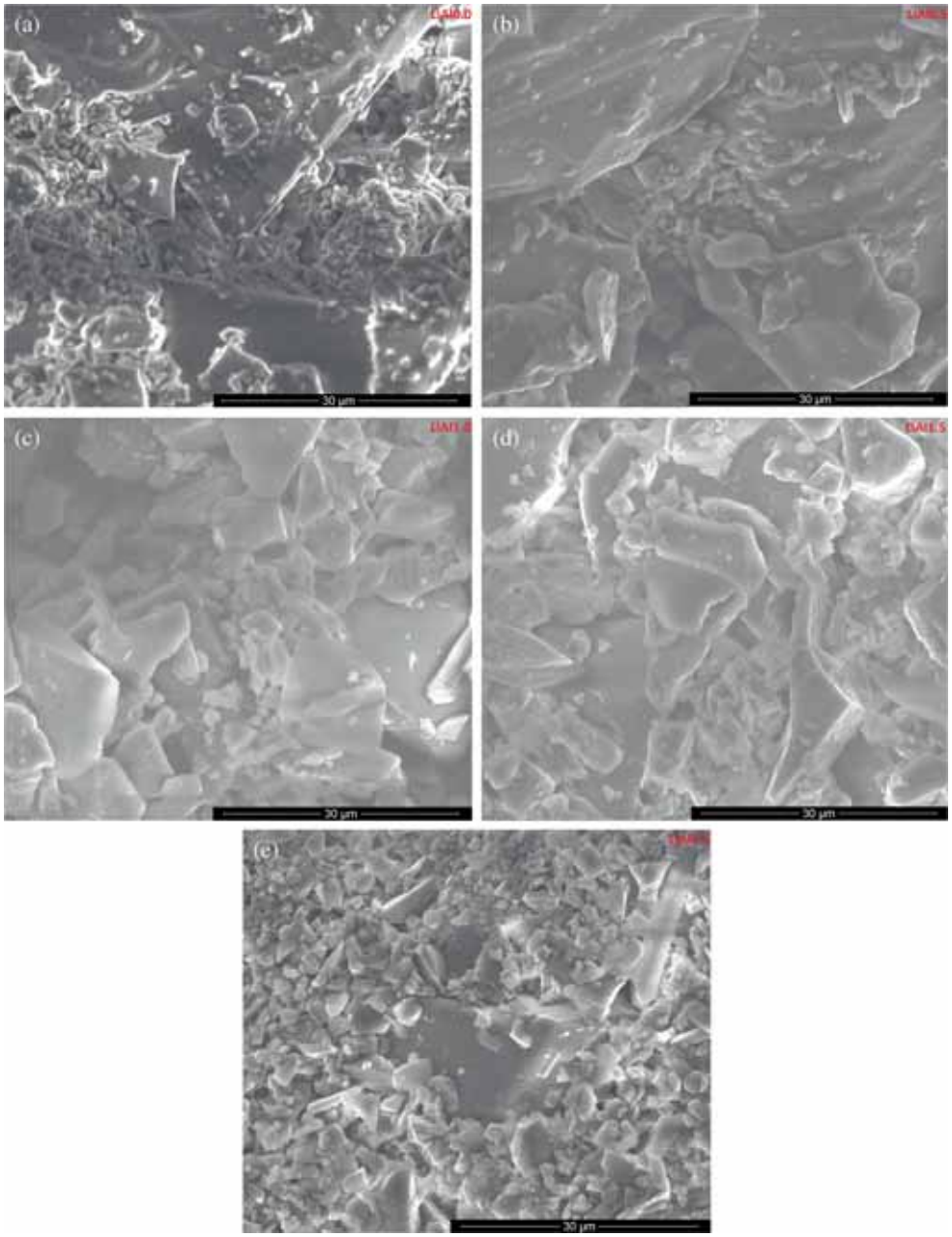

Figure 8. (**a**–**e**) SEM micrographs of bioactive glass samples before soaking in SBF solution.

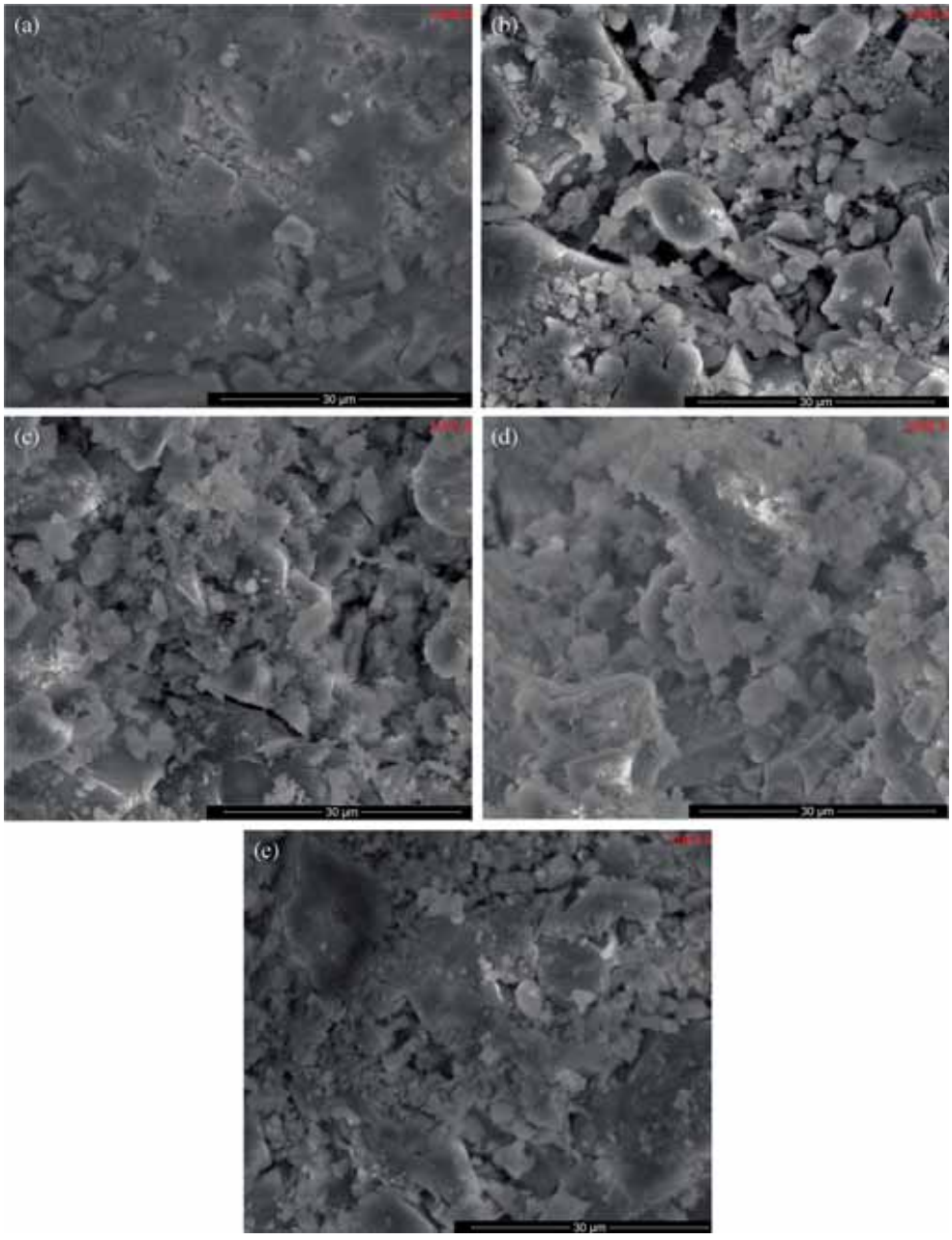

Figure 9. (**a**–**e**) SEM micrographs of bioactive glass samples which were soaked in SBF solution for 28 days.

asymmetric stretching [53,54], 748 cm^{-1} due to AlO_4 units [61] and 1990 cm^{-1} due to O–H stretching mode of vibrations. Figure 10b shows the absorption spectra of all bioglass samples after soaking into SBF solution for 1 day. The new bands were observed at 1638 and 3390 cm^{-1} in the spectra which are attributed due to presence of OH group because of water adsorption in the system [55]. Figure 10c shows the absorption spectra of all bioglass samples after soaking into SBF solution for 3 days. The spectra reveal that after soaking the samples for duration of 3 days, some additional peak was found in the spectra of bioglass samples centred at 546 cm^{-1} due to calcium phosphate (hydroxyapatite) surface layer which indicate the formation of apatite in SBF solution [56]. In addition to these other bands were also found to be centered at around 1420 and 1480 cm^{-1} which are attributed due to carbonate groups $[CO_3]^{2-}$ indicating the precipitation of B-type hydroxy carbonate apatite, $(Ca_9(HPO_4)_{0:5}(CO_3)_{0:5}(PO_4)_5OH)$ (HCA) mimicking bone-like apatite in the system [57]. Figure 10d shows the absorption spectra of all bioglass samples after soaking into SBF solution for 7 days. It is evident from the spectra that some additional bands at around 960 cm^{-1} due to P–O stretching in apatite-like structures [57] as well as 1420 and 1480 cm^{-1} due to carbonate groups $[CO_3]^{2-}$ [58] have appeared in the system as

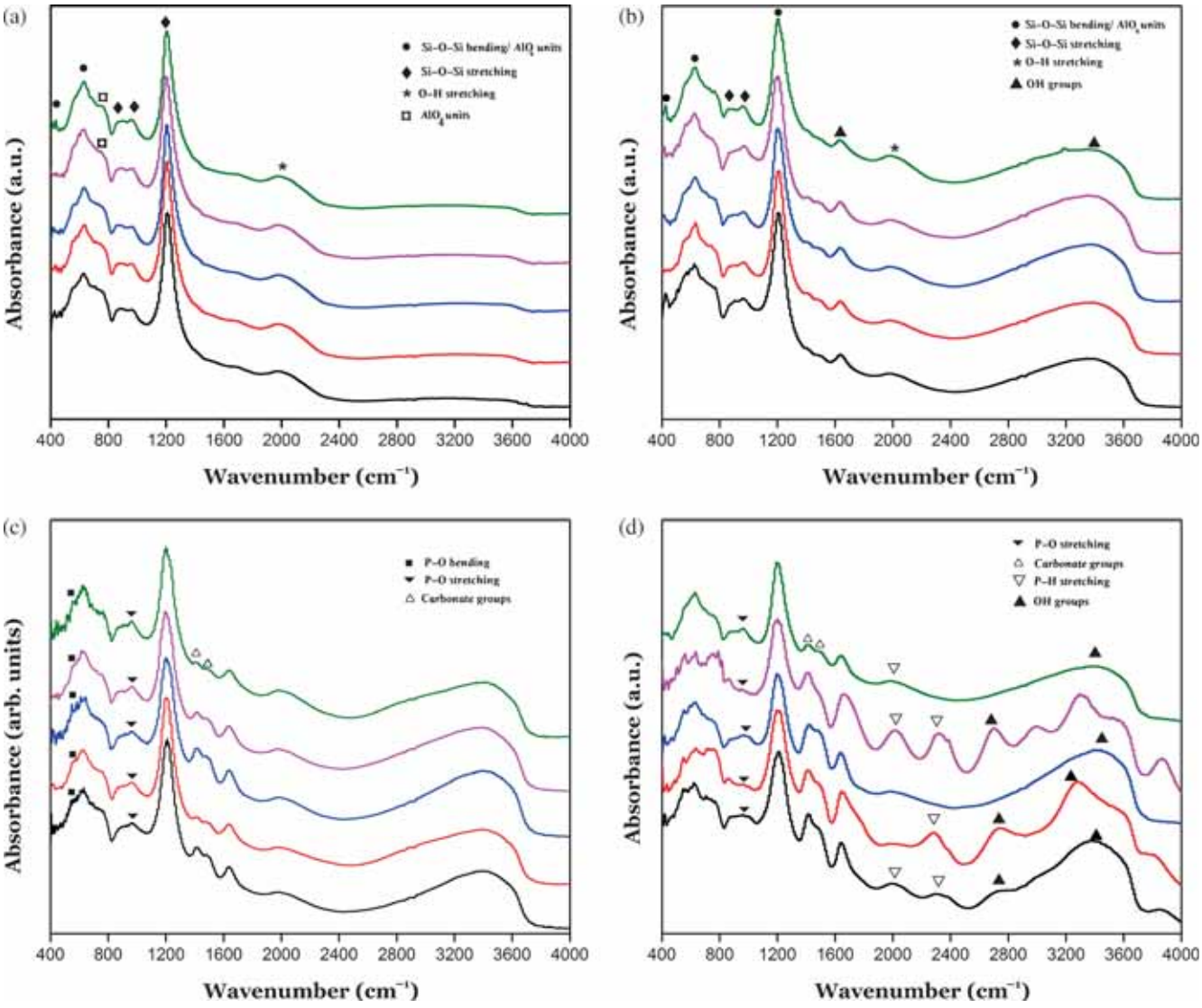

Figure 10. FTIR absorption spectra of all glass samples (**a**) before soaking them into SBF solution, (**b**) after soaking them into SBF for 1 day, (**c**) after soaking them into SBF for 3 day and (**d**) after soaking them into SBF for 7 days.

a result of SBF treatment for a period of 7 days. The absorption bands around 2010 and 2300 cm^{-1} were attributed due to P–H stretching modes as well as 2743 and 3400 cm^{-1} is due to O–H stretching mode of vibrations [57]. The formation of hydroxy carbonate apatite (HCA) layer takes place after the immersion of the samples in the SBF solution and the mechanism for the formation of HCA layer on the surface of the samples has been earlier explained by Hench in bioactive glasses [1] which bond the implant to the body bones and other tissues. The mechanism of hydroxyapatite formation followed by cation exchange involves the formation of silica-rich layer at the surface of the glass which contains Si–OH groups that act as nucleation sites for amorphous calcium–phosphate [58]. The increase in pH promotes crystallization of calcium–phosphate (Ca–P) where the tetrahedral $[PO_4]^{3-}$ exhibits sharp IR absorptions at 546 cm^{-1} characteristic to P–O bending. The absorption spectra of bioactive glass samples showed the P–O bending vibrational bands after 3 days of immersion in SBF. Other bands marked at 1420 and 1480 cm^{-1} were characteristic of carbonate group, $[CO_3]^{2-}$, indicating the precipitation of B-type hydroxy carbonate apatite (HCA), $Ca_9(HPO_4)_{0:5}(CO_3)_{0:5}(PO_4)_5OH$. The precipitation of pure hydroxyapatite in SBF is likely to happen less because it is saturated with respect to slightly carbonated apatite, in which the orthophosphates are substituted with carbonates in the crystal lattice [59]. Gibson *et al* [60] pointed out that the P–O bending bands, at 546 cm^{-1} in the FTIR spectra were not characteristic to HA or HCA, but they do indicate the presence of orthophosphate lattices. Therefore, the newly phase formed at the surface of the bioactive glass samples were also confirmed by XRD as shown in figure 7. So our results regarding formation of HCA in SBF by FTIR absorption spectrometry are well supported by the observations made by Anthony *et al* [57].

3.6 *In-vitro biocompatibility study*

The viability and cytotoxicity of bioactive glass samples was assessed using MG63 cell lines and the percent viability and cytotoxicity of the samples was measured with respect to time. The number of living cells proliferated was determined by MTT assay on the sample's surface. The optical density of the solution was measured to quantify the cell viability/living cell count. The cell viability and cytotoxicity for bioactive glass samples have been plotted as a function of time and presented in figures 11 and 12, respectively. Figures 11 and 12 clearly show a decreasing trend in cell viability and increasing in cytotoxicity with an increase in Al_2O_3 concentration beyond 1.0 mol%. Figure 11 dictates the cell viability against MG63 cell lines and the results show that the cell viability was greater than 80% even after 72 h of culture. Moreover, the bioactive glass samples such as LiAl0.0, LiAl0.5 and LiAl1.0 are comparatively less toxic than other glass samples which have been demonstrated by the inhibition of the cell viability in a time dependent manner. The present results suggest that as the concentration of alumina has increased, the cell viability was affected by bioactive glass samples, namely LiAl1.5 and LiAl2.5 (figure 11). The decrease in cell viability was also supported by growth inhibition of bioactive glass samples when the MG63 cells were cultured in presence of their varying compositions.

Similarly, the results on cell cytotoxicity demonstrated the less toxicity against osteoblast MG-63 cell lines as shown in figure 12. The bioactive glass samples; LiAl0.0, LiAl0.5 and LiAl1.0 are also less cytotoxic to MG63 cells as compared to LiAl1.5 and LiAl2.5. The cell viability and cytotoxicity results suggest that bioactive glass samples; LiAl0.0, LiAl0.5 and LiAl1.0 are relatively tolerant to MG63 cell lines in comparison to other samples like LiAl1.5 and LiAl2.5 which causes a decrease in cell viability and direct cellular cytotoxicity.

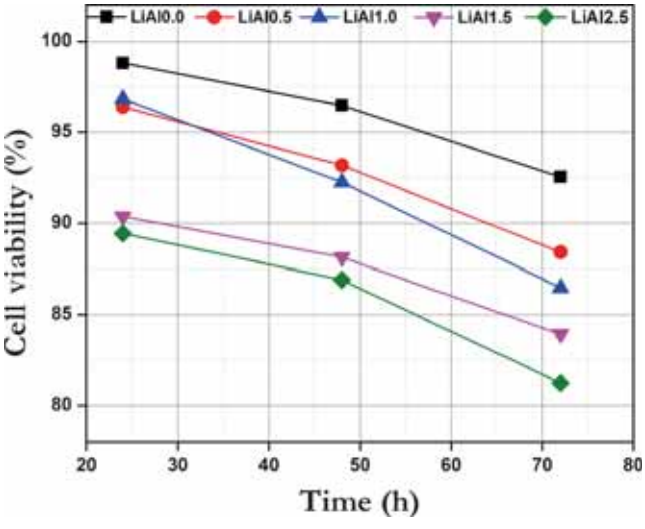

Figure 11. Viability of MG63 cells in the presence of fixed concentration (10 mg ml^{-1}) of bioactive glass samples.

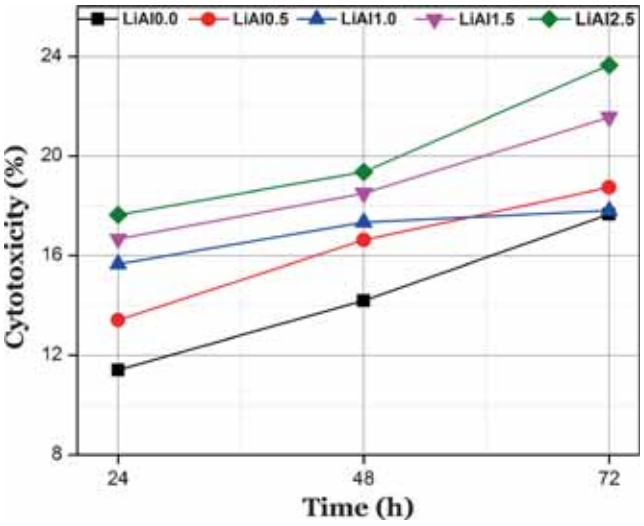

Figure 12. Cytotoxicity of MG63 cells in the presence of increasing concentrations of bioactive glass samples.

4. Conclusion

In the present investigation, a comparative study was made on bioactive, physico-chemical and mechanical properties of multi-component Li_2O–CaO–Al_2O_3–P_2O_5–SiO_2 bioactive glasses with varying concentration of Al_2O_3. The following conclusions were drawn from these investigations:

1. On increasing the amount of Al_2O_3 in the bioactive glass samples, density, compressive strength, Vickers hardness and elastic modulus were found to increase accordingly. However, the tendency towards saturation of density beyond 1.0 mol% Al_2O_3 can be due to compensating free volume increase with increasing aluminium leading to asymptotic behaviour of change in density in the glass samples.
2. The FTIR absorption spectra showed different characteristic bands because of the silicate network which indicated the formation of hydroxy carbonate apatite (HCA) layer. It is also consistent with the FTIR absorption band at around 546 cm^{-1} due to P–O bending (amorphous) as well as at 960 cm^{-1} attributed due to the formation of P–O stretching on the surface of bioactive glass samples after immersing in the SBF solution from 1 to 7 days. The present results regarding formation of HCA in SBF by FTIR absorption spectrometry are well supported by the previous observations.
3. The bioactivity of these samples was measured by *in vitro* test in SBF solution for 1–28 days. The pH of the solution was found to increase from 1 to 3 days and then it became nearly constant up to 7 days. After 7 days, the pH of the glass samples decreased which showed a decrease in the bioactivity of the samples. The mechanism of HA formation involved the SiO_2-rich layer formation at the surface of the glass samples which contained Si–OH groups acting as nucleation sites for

amorphous calcium–phosphate followed by carbonated HA.

4. The SEM analysis of pre-soaked samples in SBF showed various irregular grains of glass samples. After 28 days of SBF treatment, HCA layer was formed on the surface of these samples due to its bioactive nature. This was also confirmed by X-ray diffractometry of glass samples treated with SBF for 14 days.
5. When alumina was present in small concentrations AlO_6 octahedra dominated the glass structure, whereas AlO_4 tetrahedral units prevailed when Al_2O_3 concentration was higher. Aluminium ions occupy both tetrahedral sites with AlO_4 network former and octahedral with AlO_6 network modifier in the structure. Hence, the AlO_4 tetrahedra increases the strength of the glass and on the other hand AlO_6 octahedra increases the bioactivity of the bioglass samples.
6. The cell viability and cytotoxicity of bioactive glass samples suggest that these glasses would be useful as bioactive ceramic material which could be achieved by the modifications in molar ratios of Al_2O_3 to make them biocompatible as follows.
7. Finally, it can be concluded that the concentration of Al_2O_3 in Li_2O–CaO–Al_2O_3–P_2O_5–SiO_2 glass system should be limited up to 1.5 mol% for a proper balance between better bioactivity, physico-chemical and mechanical properties for a more suitable bioactive ceramic material.

References

[1] Hench L L 1991 *J. Am. Ceram. Soc.* **74** 1487

[2] Bohner M and Lemaitre J 2009 *Biomaterials* **30** 2175

[3] Clark A E and Hench L L 1976 *J. Biomed. Mater. Res.* **10** 161

[4] Hench L L 2006 *J. Mater. Sci. Mater. Med.* **17** 967

[5] Hench L L, Splinter R J, Allen W C and Greenlee T K 1971 *J. Biomed. Mater. Res. Symp.* **334** 117

[6] Kokubo T 1991 *Biomaterials* **12** 155

[7] LeGeros R Z 2002 *Clin. Orthop. Relat. Res.* **395** 81

[8] Cao W and Hench L L 1996 *Ceram. Int.* **22** 493

[9] Rahaman M N, Day D E, Bal B S, Fu Q, Jung S B and Bonewald L F 2011 *Acta Biomater.* **7** 2355

[10] Jung S B, Day D E, Day T, Stoecker W and Taylor P 2011 *Wound Repair Regen.* **30** 19

[11] Abou Neel E A, Pickup D M, Valappil S P, Newport R J and Knowles J C 2009 *J. Mater. Chem.* **19** 690

[12] Arstila H, Hupa L, Karlsson K H and Hupa M 2008 *J. Non-Cryst. Solids* **354** 722

[13] Shirtliff V J and Hench L L 2003 *J. Mater. Sci.* **38** 4697

[14] Li P, Zhang F and Kokubo T 1992 *J. Mater. Sci.: Mater. Med.* **3** 452

[15] Agathopoulos S, Tulaganov D U, Ventura J M G, Kannan S, Karakassides M A and Ferreira J M F 2006 *Biomaterials* **27** 1832

[16] Marti A, Dr. Robert Mathys Foundation, Bischmattstr. 12, CH-2544 Bettlach *Injury—Int. J. Care Injured* 01/2000; 31. DOI:10.1016/S0020-1383(00)80021-2

[17] El-Kheshen A, Khaliafa F A, Saad E A and Elwan R L 2008 *Ceram. Int.* **34** 1667

[18] Sitarz M, Bulat K and Szumera M 2010 *J. Non-Cryst. Solids* **356** 224

[19] Sitarz M 2010 *Eur. J. Glass Sci. Tech.* **51** 179

[20] Ohtsuki C, Kokubo T and Yamamuro T 1992 *J. Mater. Sci.: Mater. Med.* **3** 119

[21] Gross U and Strunz V 1985 *J. Biomed. Mater. Res.* **19** 251

[22] Clement-Lacroix P, Morvan F, Roman-Roman S, Vayssiere B and Belleville C 2005 *Proc. Natl. Acad. Sci.* **102** 17406

[23] Zamani A, Omrani R G and Nasab M M 2009 *Bone* **44** 331

[24] Kokubo K, Ito S, Huang Z T, Hayashi T, Sakka S, Kitsugi T and Yamamuro T 1990 *J. Biomed. Mater. Res.* **24** 721

[25] Kapusetti G, Misra N, Singh V, Srivastava S, Roy P, Dana K *et al* 2014 *J. Mater. Chem. B.* **2** 3984

[26] Kapusetti G, Misra N, Singh V, Kushwaha R K and Maiti P 2012 *J. Biomed. Mater. Res. A* **100** 3363

[27] Shannon R D 1976 *Acta Crystallogr. Sect. A* **32** 751

[28] Scholes S R 1975 *Modern Glass Practice* (Boston, MA: Cahners Books) 7th ed., p 375

[29] Andersson O H and Sodergard A 1999 *J. Non-Cryst. Solids* **246** 9

[30] Branda F, Costantini A, Luciani G and Laudisio G 2001 *J. Ther. Analy. Calori.* **64** 1017

[31] Mirhadia B and Mehdikhanib B 2012 *N. J. Glass Ceram.* **2** 1

[32] Vallet-Reg M, Roma J, Padilla S, Doadrio J C and Gil F J 2005 *J. Mater. Chem.* **15** 1353

[33] Paul A 1990 *Chemistry of Glasses* (London: Chapman & Hall) 2nd ed., p 149–151

[34] Varshneya A K 2006 *Fundamentals of Inorganic Glasses* (Sheffield, UK: Society of Glass Technology) p 129, 515–17

[35] Paul A and Zaman M S 1978 *J. Mater. Sci.* **13** 1499

[36] Teixeira Z, Alves O L and Mazali I O 2007 *J. Am. Ceram. Soc.* **90** 256

[37] Filguei Ras M R, LaTorre G and Hench L L 1993 *J. Biomed. Mater. Res.* **27** 1485

[38] Belkebir A, Rocha J, Esculcas A P, Berthet P, Gilbert B and Gabelica Z 1999 *Spectrosc. Acta* **55** 1323

[39] Muller D, Berger G, Grunze I, Ludwig G, Hallas E and Haubenreisser U 1983 *Phys. Chem. Glasses* **24** 37

[40] Brow R K and Tallant D R 1997 *J. Non-Cryst. Solids* **222** 396

[41] Greenspan D C and Hench L L 1976 *J. Biomed. Mater. Res.* **10** 503

[42] Hayakawa S, Tsuru K, Ohtsuki C and Osaka A 1999 *J. Am. Ceram. Soc.* **82** 2155

[43] Kasuga T, Hosoi Y, Nogami M and Niinomi M 2001 *J. Am. Ceram. Soc.* **84** 45

[44] Filgueitras M R, LaTorre G and Hench L L 1993 *J. Biomed. Mater. Res.* **27** 1485

[45] Majhi M R, Pyare R and Singh S P 2012 *J. Biomater. Tissue Eng.* **2** 1

[46] Majhi M R, Pyare R and Singh S P 2011 *J. Biomim. Biomater. Tissue Eng.* **11** 45

[47] Majhi M R, Kumar R, Singh S P and Pyare R 2011 *J. Biomim. Biomater. Tissue Eng.* **12** 1

[48] de Groot K, Wolke J G C and Jansen J A 1998 *Proc. Int. Mech. Eng.* **212** 137

[49] Vitale Brovarone C, Verne E and Appendino P 2006 *J. Mater. Sci.: Mater. Med.* **17** 1069

[50] Beherei H H, Mohamed K R and El-Bassyouni G T 2009 *Ceram. Int.* **35** 1991

[51] Nakamura M, Mochizuki Y, Usami K, Itoh Y and Nozaki T 1984 *Solid State Commun.* **50** 1079

[52] Kusabiraki K 1986 *J. Non-Cryst. Solids* **79** 208

[53] Goh Y-F, Alshemary A Z, Akram M, Rafiq M Kadir A and Hussain R 2014 *Ceram. Int.* **40** 729

[54] Cerruti M, Greenspan D and Powers K 2005 *Biomaterials* **26** 1665

[55] Stoch A, Jastrzebski W, Brozek A, Trybalska B, Cichocinska M and Szarawara E 1999 *J. Mol. Struct.* **511–512** 287

[56] ElBatal H A, Azooz M A, Khalil E M A, Soltan Monem A and Hamdy Y M 2003 *Mater. Chem. Phys.* **80** 599

[57] Macon A L B, Kim T B, Valliant E M, Goetschius K, Brow R K, Day D E, Hoppe A, Boccaccini A R, Kim I Y, Ohtsuki C, Kokubo T, Osaka A, Vallet-Regı' M, Arcos D, Fraile L, Salinas A J, Teixeira A V, Vueva Y, Almeida R M, Miola M, Vitale-Brovarone C, Verne E, Holand W and Jones J R 2015 *J. Mater. Sci.: Mater. Med.* **26** 115

[58] Kutbay I, Yilmaz B, Evis Z and Usta M 2014 *Ceram. Int.* **40** 14817

[59] Elliot J C ed 1994 *Structure and Chemistry of the Apatites and Other Calcium Orthophosphates* (Amsterdam: Elsevier Science)

[60] Gisbon I R, Rehman I, Best S M and Bonfield W 2000 *J. Mater. Sci.* **12** 799–804

[61] Mohini G J, Krishnamacharyulu N, Baskaran G S, Rao P V and Veeraiah N 2013 *Appl. Surf. Sci.* **287** 46